A Systematic Approach for Lifetime Evaluation of PV-Battery Systems

Sandelic, Monika; Sangwongwanich, Ariya; Blaabjerg, Frede

Published in:
Proceedings of IECON 2019 - 45th Annual Conference of the IEEE Industrial Electronics Society

DOI (link to publication from Publisher):
10.1109/IECON.2019.8927586

Creative Commons License
Unspecified

Publication date:
2019

Document Version
Accepted author manuscript, peer reviewed version

A Systematic Approach for Lifetime Evaluation of PV-Battery Systems

Monika Sandelic, Ariya Sangwongwanich, Frede Blaabjerg
Department of Energy Technology, Aalborg University, Aalborg DK-9220, Denmark
mon@et.aau.dk, ars@et.aau.dk, fbl@et.aau.dk

***Abstract*—Battery energy storage systems (BESS) have recently been widely integrated to photovoltaic (PV) systems with the aim of increasing the control flexibility. To ensure the profitability under long-term operation of PV-BESS, lifetime evaluation is necessary during the design stage. In PV-BESS, the battery and power converters are the reliability-critical components that are subjected to high stress during the operation. This paper proposes a systematic lifetime evaluation framework for the PV-BESS where a three-stage modeling approach is applied to the battery and power converter lifetime estimation. The proposed lifetime evaluation also includes the interaction between the operation of the battery and power converter and its impact on the lifetime, which is the key novelty of this work. The framework is demonstrated on a case study of the PV-BESS in Germany. It reveals that the battery is the most life-limiting component, where the deep cycles and high average state-of-charge are the main factors limiting the battery lifetime. Additionally, the thermal stress of the battery converter is higher than that of the PV converter due to the high loading dynamic resulting from the battery charging/discharging.**

***Index Terms*—Photvoltaic system, battery, DC/DC converters, lifetime, reliability, mission profile**

I. Introduction

The penetration of photovoltaic (PV) technology has been increasing with a fast pace in recent years, and more installations are expected in the future. This is reflected by the highest growth rate compared to other types of energy technology [1]. The power generated by PV systems is intermittent by its nature, which is strongly dependent on the solar irradiance and temperature of the installation site. This limited power control flexibility can raise challenges in terms of grid-integration. In order to mitigate this issue, integrating energy storage systems into PV systems is considered to be a promising solution, and has already been adopted commercially [2]. Among various available energy storage technologies, battery energy storage systems (BESS), especially the ones based on the Lithium-ion technology, have been widely adopted in PV applications [3], [4]. This is due to their merits of fast response time, high efficiency, low self-discharge rate and the scalability due to a modular structure. Moreover, the cost of Lithium-ion batteries has been declining significantly over the past years [5]–[7].

Inevitably, the benefit of BESS integration comes with price of higher initial investment (compared to the PV systems). Thus, in order to ensure the economic profitability under long-term operation and the system reliability (availability), the lifetime evaluation becomes a crucial task during the system design. In general, for the PV-BESS, the power processing unit consists of three main components: 1) PV panels, 2) battery systems, and 3) power electronic systems. The PV panel lifetime could reach up to 25 years - considering the typical degradation rate and warranty period [8]. On the other hand, the batteries and the power electronic systems (e.g., DC/DC converters and DC/AC inverter) can degrade/wear-out with a much faster rate, and typically need to be replaced a few times during the entire lifespan of the PV systems. Thus, they are considered as the life-limiting components in the PV-BESS.

According to the previous study [9], battery lifetime is strongly dependent on the application-specific operating conditions, where component sizing has a strong influence. In [6] and [10], the lifetime models of batteries have been developed and applied to grid-support applications. Similar research has been done in the PV application [9], and an optimal sizing approach has been proposed in [11], [12]. The lifetime modeling approach for power electronics in PV application (e.g., PV inverters) has also been discussed in [13], [14], where the impact of the operating condition on the inverter lifetime has been investigated in several aspects (e.g., installation site, PV panel degradation, and PV panel sizing). However, in those studies, the influence of the battery operation on the power electronics lifetime has not been taken into consideration. In fact, recent study in [15] has shown that the operational strategy and the sizing of the battery systems can strongly affect the loading condition and, thus, the reliability of the power electronics in PV-BESS. Hence, the operation of BESS will not only affect the lifetime of the batteries, but also the power electronic systems in PV-BESS. Without taking into account both components (i.e., the lifetime of batteries and power electronics), the overall lifetime performance of the PV-BESS cannot be ensured. This aspect has not yet been taken into consideration in the literature.

In order to fill out this gap, this paper proposes a systematic approach for lifetime evaluation of PV-BESS. The novelty of this paper lies in the comprehensive lifetime assessment of the entire PV-BESS, where the reliability-dependency of the batteries and power electronic systems is taken into consideration during the modeling. A step-by-step procedure for the lifetime assessment of each critical component is presented considering the major failure mechanisms and their stress factors. In fact, seen from the lifetime modeling perspective, the procedure for lifetime estimation of batteries and power electronics share certain similarities, which can simplify the modeling process

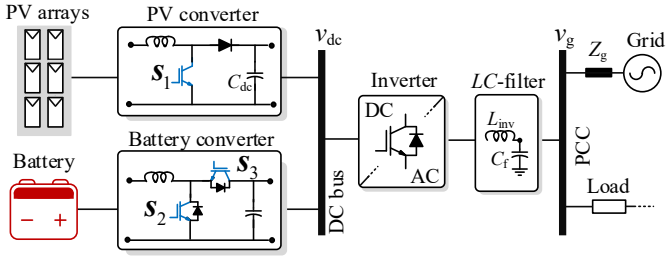

Fig. 1. System diagram of the single-phase PV-BESS in a DC coupled configuration.

considerably. That aspect will also be highlighted in this paper.

With respect to that, an overview of the system under study and an implemented energy management strategy (EMS) are given in Section II. The lifetime estimation framework with a step-by-step procedure for the lifetime assessment of the critical components in PV-BESS application is presented in Section III. The proposed framework is applied as the study case in Section IV, and concluding remarks are given in Section V.

II. Description of the PV-Battery Systems

A. PV-BESS Configuration

A system diagram of a single-phase PV-BESS is shown in Fig. 1, and the key parameters are provided in Table I. The system represents DC-coupled configuration, where the PV and the BESS are connected to the same DC bus through the interface of DC/DC power converters. The PV panel is connected to the PV converter (i.e. boost converter), which consists of two identical units connected in parallel to achieve the required power rating. The PV converter is employed to step up the PV panel output voltage to the required DC-link voltage level. It is also responsible to always extract the maximum available PV power [13]. The BESS consists of a battery connected to the battery converter (e.g., bidirectional buck-boost converter). Depending on the BESS operation, the converter operates either in the boost (e.g., during BESS discharging) or buck (e.g., during BESS charging) mode. The power at the DC-link is then transferred through the PV inverter (e.g., DC/AC inverter) to the grid or to supply the load.

B. Energy Management Strategy (EMS)

There are several EMS that can be applied to PV-BESS. Among others, self-consumption is predominantly adopted commercially in the residential-scale PV-BESS (e.g., the one in Fig. 1) [3]. The key target of self-consumption is to maximize the use of PV power generation for the local load supply, while the battery is used to absorb/supply the power mismatch between the two. Considering that, the requested power for the battery can be summarized as:

$$P_{BESS\_req} = P_{PV} - P_{load} \tag{1}$$

where P_{BESS_req} is the battery requested power, P_{PV} is the PV power, and P_{load} is the load demand.

TABLE I
Parameters of the Single-Phase PV-BESS.

PV array rated power (at STC)	6 kW
PV converter rated power	6 kW (3 kW x 2 units)
Battery energy capacity	7.5 kWh
Battery converter rated power	3 kW
Inverter rated power	6 kW
DC-link capacitor	C_{dc} = 1100 μF
LC-filter	L_{inv} = 4.8 mH, C_f = 4.3 μF
Switching frequency	DC/DC Converters: f_{sw} = 20 kHz
DC-link voltage	v^*_{dc} = 450 V
Grid nominal voltage (RMS)	V_g = 230 V
Grid nominal frequency	ω_0 = 2$\pi\times$50 rad/s

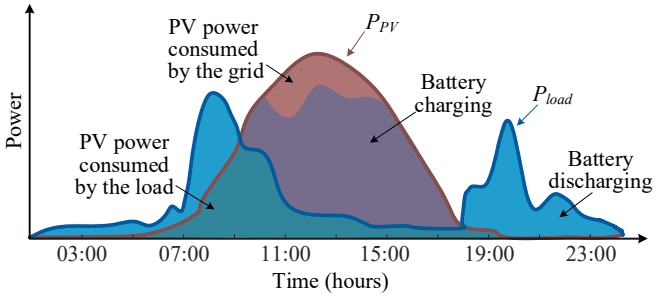

Fig. 2. A typical daily profile with PV power generation and implemented self-consumption strategy, where P_{PV} is the PV power and P_{load} is the load demand.

When the battery is fully charged, the surplus PV power is delivered to the grid. On the other hand, the load will be supplied by the grid when the PV power is not available and the battery is fully discharged. A graphical representation of a typical daily profile based on the self-consumption strategy is shown in Fig. 2.

III. Proposed Lifetime Estimation Framework

In this section, a framework for lifetime estimation based on the step-by-step procedure is presented. Firstly, it is necessary to identify the main life-limiting components, their failure mechanisms (and stress factors), and the relevant lifetime models. Although the power electronics and batteries have different failure mechanisms, the approach for the lifetime evaluation is to a certain extent similar, as it is summarized in Table II. Therefore, the modeling stages of the proposed lifetime framework are defined as 1) mission profile translation to stress profiles, 2) stress profiles interpretation and 3) lifetime prediction. The overview of the framework is given in Fig. 3.

For the power electronics, the lifetime model is based on the wear-out failure mechanism of power devices, e.g., Insulated-Gate Bipolar Transistor (IGBT), related to thermal stress conditions. In general, the thermal cycling and the mean junction temperature of the device have major contribution to the lifetime of the IGBT (e.g., bond-wire lift off). In the case of the batteries, the main degradation mechanism is related to the loss of electrolyte, which is directly reflected in the decreased capacity, where the state-of-charge (SOC) is the most relevant

TABLE II
SUMMARY OF THE FAILURE MECHANISMS AND LIFETIME MODELING APPROACH FOR POWER ELECTRONICS AND BATTERY.

Component	Failure Mechanisms	Stress Factors	Lifetime Model
Power device (e.g., IGBT)	bond wire lift-off, solder fatigue	Junction temperature T_j	$N_f(\Delta T_j, T_{jm}, t_{on})$
Battery	loss of electrolyte, depletion of active chemicals	State-of-charge SOC	$C_f(\Delta SOC, SOC_m, N_c, t_l)$

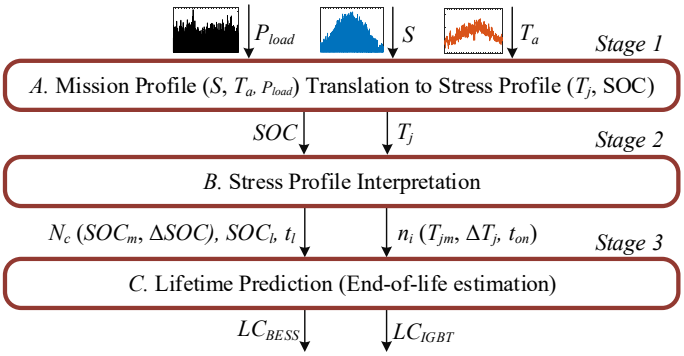

Fig. 3. Overview of the proposed lifetime estimation framework of PV-BESS with three modeling stages. Input variables are load demand P_{laod}, solar irradiance S and ambient temperature T_a. Investigated stress profiles are state-of-charge SOC and junction temperature of the power device T_j. The output variables are lifetime consumption of power device LC_{IGBT} and battery LC_{BESS}.

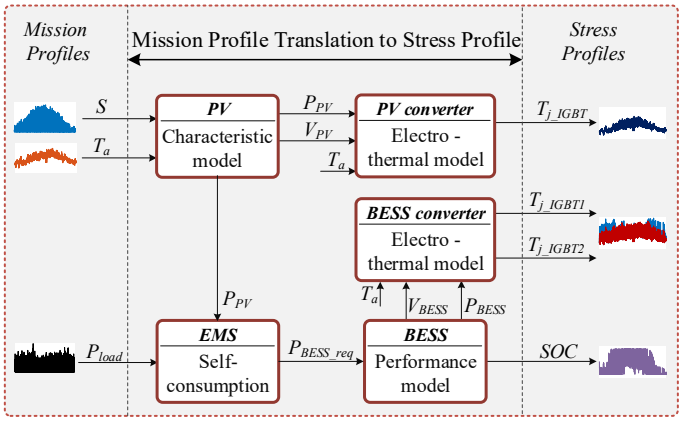

Fig. 4. Flow chart of mission profile translation to stress profile where the input mission profiles are solar irradiance S, ambient temperature T_a and load profile P_{load}, and the output stress profiles are IGBT junction temperature T_j and battery state-of-charge SOC.

stress factor. This can be further divided into two main stress conditions related to the cycling and idling (standby) operation of the batteries. In both cases, the stress profile (e.g., junction temperature of the power device or SOC of the battery) needs to be obtained from the real operating conditions, referred to as a mission profile. With respect to that, mission profile is the input to Stage 1 of the process. In Stage 2, the obtained stress profiles are decomposed and organized in a form suitable for characteristic lifetime models. By performing Stage 3, an estimation of lifetime consumption (LC) is obtained by means of lifetime models based on the empirical data. Each modeling stage will be elaborated in the following.

A. Mission Profile Translation to Stress Profile (Stage 1)

An overview of Stage 1 is shown in Fig. 4 where the mission profiles of PV-BESS are the solar irradiance S, the ambient temperature T_a, and the load profiles P_{load}. Normally, a yearly profile is used in order to take the seasonal variation in the environmental conditions and load demand into account. In order to translate the mission profile into the relevant stress profiles of the components under study, the following models are needed.

1) PV Model: The PV panel electrical characteristic model presented in [16] is used to obtain the power generated by the PV at the maximum power point P_{PV} and the associated voltage V_{PV} under a given solar irradiance S and ambient temperature T_a conditions. Those parameters (i.e., PV power and voltage) are used as input of the PV converter model, since they determine the power loading and the efficiency of the converter.

2) Battery Model: The battery model is required to obtain the SOC stress profile. The power requested from the battery, P_{BESS_req} is determined by following (1) i.e., from the self-consumption control strategy with considered the PV power and the load profiles. The actual power from the battery, P_{BESS} is determined based on the requested power, current SOC and its limitations. To determine the associated SOC level, a SOC estimator based on the Coulomb counting implemented in the performance model developed in [17] is used. In order to assure safe and prolonged BESS operation, SOC is limited between 10% and 90%, as recommended in [18].

3) Power Electronics Models: The electro-thermal model of power converter is required to obtain the thermal loading of the power devices. This is done by taking into account the power losses of the IGBT (e.g., conduction and switching losses) under a certain operating power, voltage, and temperature conditions. Then, the IGBT junction temperature T_j is obtained by applying the power losses into the thermal model of the power device. By doing so, the junction temperature profile under the mission profile operation can be obtained and used in the stress profile interpretation. This is applied for both the PV and the battery converter.

B. Stress Profile Interpretation (Step 2)

The stress profiles T_j and SOC, obtained from the previous step, are irregular profiles (with different depth and duration of each cycle) due to the mission profile dynamics. In order to extract the cycling distribution, which is required as an input parameter of the lifetime model, a cycle counting method needs to be applied. Accordingly, the rainflow cycle counting

TABLE III
PARAMETERS OF THE LIFETIME MODEL OF AN IGBT.

Parameter	Value	Experimental condition
A	3.4368×10^{14}	
α	-4.923	$64\ \text{K} \leq \Delta T_j \leq 113\ \text{K}$
β_1	-9.012×10^{-3}	
β_0	1.942	$0.19 \leq ar \leq 0.42$
C	1.434	
γ	-1.208	$0.07\ \text{s} \leq t_{on} \leq 63\ \text{s}$
f_d	0.6204	
E_a	0.06606 eV	$32.5\ ^\circ\text{C} \leq T_j \leq 122\ ^\circ\text{C}$
k_B	8.6173324×10^{-5} eV/K	

algorithm is commonly used to extract the cycle information such as the cycle amplitude, the mean value, and the cycle period [19], [20]. By applying this method to both - the battery SOC and the IGBT junction temperature profiles, the number of cycles under a given cycle amplitude, mean value, and cycle period are obtained. The outputs of the rainflow algorithm can then be applied to the lifetime models.

C. Lifetime Prediction (Step 3)

Lifetime models in general provide the information of the component capability to withstand the stress (e.g., number of cycles to failure) under a given operating condition. For the IGBTs, temperature-related lifetime model typically represents the bond-wire lift off failure mode (and solder degradation), which can be expressed as follows [13]:

$$N_f = A \cdot (\Delta T_j)^{\alpha} \cdot (ar)^{\beta_1 \Delta T_j + \beta_0} \cdot \left[\frac{C + (t_{on})^{\gamma}}{C+1}\right] \cdot \exp\left(\frac{E_a}{k_b \cdot T_{jm}}\right) \cdot f_d \quad (2)$$

where N_f is the number of cycles to failure under the stress condition of the mean junction temperature T_{jm}, the cycle amplitude ΔT_j and the cycle period t_{on}. The rest of the parameters are provided in Table III. Then, the Miner's rule is used to express the amount of device life that is consumed during operation LC_{IGBT}, which is defined as:

$$LC_{IGBT} = \sum_i \frac{n_i}{N_{fi}} \quad (3)$$

where n_i is the number of cycles for a certain set of values of T_{jm}, ΔT_j and t_{on} and N_{fi} is the number of cycles to failure obtained from (2). When the LC_{IGBT} is accumulated to 1, the IGBT is considered to reach its end-of-life (EOL).

In the case of the batteries, LC_{BESS} is defined as the reduction of its capacity. Expression for capacity fade is defined as follows:

$$C_f = a_{cyc} \cdot N_c(\Delta SOC)^{b_{cyc}} + a_{idl} \cdot k_T \cdot k_V \cdot t_l \quad (4)$$

where the first term represents the capacity fade C_f under the cycling stress condition where a_{cyc} is the function of the mean SOC, SOC_m and the cycle amplitude, ΔSOC while $N_c(\Delta SOC)$ represents the equivalent full cycles that are determined by means of Wöhler function. The second part

TABLE IV
PARAMETERS OF THE LIFETIME MODEL OF BATTERY.

Parameter	Value	Description
b_{cyc}	1	Cycle aging parameter
a_{idl}	6.6269×10^{-4}	Idle aging parameter
a_w	151245.25	Wöhler parameter
b_w	-0.968423	Wöhler parameter

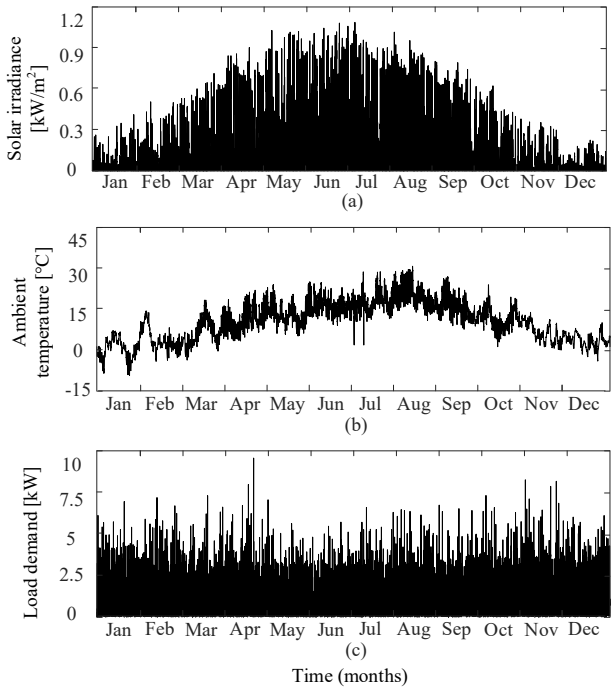

Fig. 5. One-year mission profile of the PV-BESS in Lindenberg, Germany with a sampling rate of 5 minutes per sample: (a) Solar irradiance, (b) Ambient temperature, and (c) Household load profile.

of the equation represent the capacity fade C_f under the idling stress conditions where k_T and k_V represent the Arrhenius and Tafel equation respectively and t_l represents associated time the battery spent idling. The rest of the parameters are provided in Table IV while detailed explanations of the used lifetime model are provided in [3].

Finally, the lifetime consumption of the battery during operation is calculated as:

$$LC_{BESS} = \sum_i C_{fi} \quad (5)$$

where C_{fi} is the capacity fade for the certain operating conditions reflected in the SOC stress profile. From the LC, it is possible to determine the battery state-of-health which accounts for 1 when LC equals zero. The battery has reached its EOL when LC_{BESS} accumulates to 1 which corresponds to 20% capacity fade.

IV. CASE STUDY

In order to demonstrate the proposed three-stage lifetime evaluation procedure, a case study for the PV-BESS with the

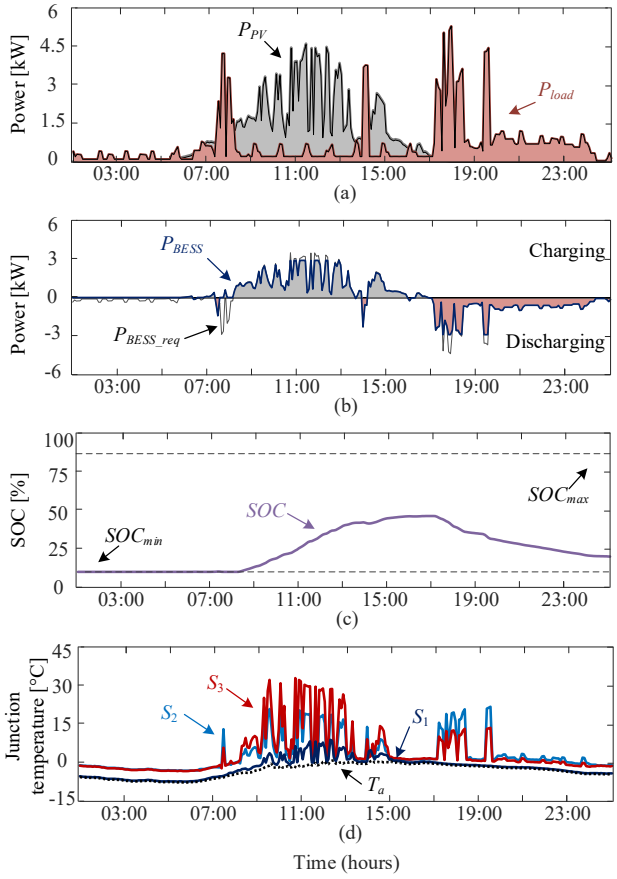

Fig. 6. One-day profiles of the PV-BESS: (a) PV and load power, (b) Requested and available battery power, (c) Battery SOC, and (d) Junction temperature of the power devices of PV converter (one 3 kW unit) and battery converter.

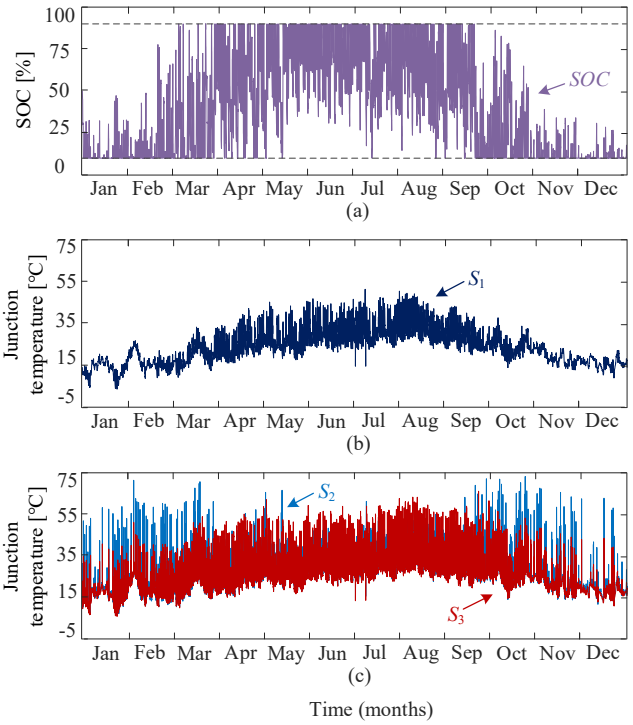

Fig. 7. Stage 1 output one-year stress profiles: (a) Battery SOC, (b) Junction temperature of PV converter (one 3 kW unit) power device S_1, and (c) Junction temperature of battery converter power devices - S_2 and S_3.

installation site at Lindenberg in Germany is carried out. The system configuration and the parameters have been discussed in Section II and the focus is on the lifetime of the battery, the battery converter, and the PV converter.

A. Mission Profiles

The solar irradiance and ambient temperature (Fig. 5) are measured with a sampling rate of 5 minutes per sample. The load profile of a typical four-member household with an average yearly consumption of 4.8 kWh/year is also used as the input and it is generated by using a tool described in [21].

B. Stress Profiles

In order to demonstrate the self-consumption control strategy, a one-day operation is first investigated where the PV power generation P_{PV} and load demand P_{load} are shown in Fig. 6(a). The difference between the two aforementioned profiles indicates the requested power for the BESS unit P_{BESS_req}, while the actual BESS power, P_{BESS} also needs to take into consideration the battery power and energy capacity limits. This can be observed in Fig. 6(b) where the requested power and available power differs when the requested power exceeds the battery nominal power of 3 kW or when the SOC reaches its limits (as shown in Fig. 6(c)). The junction temperatures of the IGBTs of the PV and battery converter are also provided in Fig. 6(d). The variation of the junction temperature of the IGBTs S_2 and S_3 in the battery converter are strongly influenced by the battery operation. More specifically, during the battery discharging, the thermal loading of the IGBT S_2 (marked in Fig. 1) is higher than that of S_3 since the battery converter operates in the boost mode. In contrast, the thermal loading of the IGBT S_3 is increased during the battery charging. The loading of the PV converter follows the dynamics of PV power generation, which is equally distributed to two 3 kW units connected in parallel. This results in lower loading conditions for each PV converter unit compared with the battery converter and lower junction temperature of the IGBT S_1.

When the operation under the mission profile in Fig. 5 is considered, four stress profiles (i.e., SOC of the battery and junction temperature of IGBTs of DC/DC converters) are obtained and they are shown in Fig. 7. As it can be seen from Fig. 7(a), the battery tends to cycle closer to the lower SOC limit during the winter period. In contrast, the SOC with deeper cycles is closer to the upper SOC limit during the summer period. The junction temperatures of the IGBTs S_2 and S_3 are also affected by the battery operation. This is due to the battery SOC and voltage dependency. For lower SOC level, the battery voltage will also be low, and thus the battery converter needs to operate with high step-up ratio. This

TABLE V
ESTIMATED LIFETIME CONSUMPTION OF IGBTS AND BATTERY FOR ONE-YEAR MISSION PROFILE SHOWN IN FIG. 5.

Component	LC after one year
PV converter (single 3 kW unit) - S_1	0.06×10^{-1}
Battery converter - S_2	0.48×10^{-1}
Baterry converter - S_3	0.22×10^{-1}
Battery	1.71×10^{-1}

usually introduces more power losses in the IGBT, which is then reflected in the higher junction temperature, as it can be seen in Fig. 7(c). In contrast, the thermal stress of the IGBT S_1 is subjected to lower variations in cycle magnitude than the IGBTs of the battery converter. This is mainly due to a more variable power flow imposed to battery unit.

C. Lifetime Consumption

The stress profiles in Fig. 7 are applied to the cycle counting algorithm (i.e., Stage 2) and the outputs are used for the lifetime assessment (i.e., Stage 3). The summary of the lifetime evaluation results is shown in Table V. It can be observed that the battery has the highest LC among all the considered components in PV-BESS, and it will experience the shortest operating lifetime. It is concluded that the cycling at high average SOC has the highest contribution to the capacity fade and is limiting the lifetime of the battery. Lifetime of the Battery converter is determined based on the lifetimes of the IGBTs S_2 and S_3, while PV converter lifetime is influenced by the lifetime of the IGBT S_1 in each of the 3kW units. With that respect, battery converter has shorter lifetime than the PV converter.

Finally, it is worth mentioning that the presented lifetime assessment can further be extended to perform reliability studies of the complete system. In that case, the system-level assessment should be carried out, where the lifetime evaluation method discussed in this paper should be implement with a probabilistic approach (e.g., Monte-Carlo simulation).

V. CONCLUSION

In this paper, a framework for the lifetime estimation of the PV-BESS is presented, where the lifetime of the battery and power electronics are considered. In fact, both the battery and the power electronics share similar lifetime evaluation procedure although their degradation mechanisms, stress factors, and lifetime models are different. Thus, this paper demonstrates that the lifetime evaluation of the each component can be done together in a systematic way, where the operational impact of each component and the interaction (e.g., loading) are included in the analysis. A case study of the PV-BESS installed in Germany reveals that the battery is the most critical component in terms of lifetime. By using the proposed framework, the lifetime information of the critical components (such as battery and power electronics) can be obtained and used in the planning stage of the PV-BESS.

REFERENCES

[1] REN21, "Renewables 2018: Global Status Report (GRS)," 2019. [Online]. Available: http://www.ren21.net

[2] SMA Solar Technology AG, "Planning guidelines - the system solution for more independence," 2013. [Online]. Available: https://files.sma.de/dl/1353/SI-HoMan-PL-en-51.pdf

[3] G. Angenendt, S. Zurmühlen, H. Axelsen, and D. U. Sauer, "Comparison of different operation strategies for PV battery home storage systems including forecast-based operation strategies," *Applied Energy*, vol. 229, pp. 884 – 899, 2018.

[4] H. Beltran, I. Tomás García, J. C. Alfonso-Gil, and E. Pérez, "Levelized cost of storage for Li-Ion batteries used in PV power plants for ramp-rate control," *IEEE Trans. Energy Convers.*, vol. 34, no. 1, pp. 554–561, Mar. 2019.

[5] World Energy Council, "E-storage: Shifting from cost to value - wind and solar applications," 2016. [Online]. Available: https://www.worldenergy.org

[6] D. Stroe, M. Swierczynski, A. Stroe, R. Laerke, P. C. Kjaer, and R. Teodorescu, "Degradation behavior of lithium-ion batteries based on lifetime models and field measured frequency regulation mission profile," *IEEE Trans. Ind. App.*, vol. 52, no. 6, pp. 5009–5018, Nov. 2016.

[7] H. Hesse, M. Schimpe, D. Kucevic, and A. Jossen, "Lithium-ion battery storage for the grid—a review of stationary battery storage system design tailored for applications in modern power grids," *Energies*, vol. 10, no. 12, pp. 2107–2149, 2017.

[8] National Renewable Energy Laboratory (NREL), "On the path to sunshot: The role of advancements in solar photovoltaic efficiency, reliability, and costs," Tech. Rep. No. NREL/TP-6A20-65872, 2016.

[9] G. Angenendt, S. Zurmühlen, R. Mir-Montazeri, D. Magnor, and D. U. Sauer, "Enhancing battery lifetime in PV battery home storage system using forecast based operating strategies," *Energy Procedia*, vol. 99, pp. 80 – 88, 2016.

[10] D. Stroe, M. Świerczyński, A. Stan, R. Teodorescu, and S. J. Andreasen, "Accelerated lifetime testing methodology for lifetime estimation of lithium-ion batteries used in augmented wind power plants," *IEEE Trans. Ind. App.*, vol. 50, no. 6, pp. 4006–4017, Nov. 2014.

[11] J. Weniger, T. Tjaden, and V. Quaschning, "Sizing of residential PV battery systems," *Energy Procedia*, vol. 46, pp. 78 – 87, 2014.

[12] G. Merei, J. Moshövel, D. Magnor, and D. U. Sauer, "Optimization of self-consumption and techno-economic analysis of PV-battery systems in commercial applications," *Applied Energy*, vol. 168, pp. 171 – 178, 2016.

[13] A. Sangwongwanich, Y. Yang, D. Sera, F. Blaabjerg, and D. Zhou, "On the impacts of PV array sizing on the inverter reliability and lifetime," *IEEE Trans. Ind. App.*, vol. 54, no. 4, pp. 3656–3667, Jul. 2018.

[14] A. Sangwongwanich, Y. Yang, and F. Blaabjerg, "Development of flexible active power control strategies for grid-connected photovoltaic inverters by modifying mppt algorithms," in *Proc. of IFEEC 2017 ECCE Asia*, Jun. 2017, pp. 87–92.

[15] A. Sangwongwanich, G. Angenendt, S. Zurmuhlen, Y. Yang, D. Sera, D. U. Sauer, and F. Blaabjerg, "Enhancing PV inverter reliability with battery system control strategy," *CPSS Trans. Power Electron. Appl.*, vol. 3, no. 2, pp. 93–101, Jun. 2018.

[16] D. Sera, R. Teodorescu, and P. Rodriguez, "PV panel model based on datasheet values," in *Proc. of ISIE*, Jun. 2007, pp. 2392–2396.

[17] M. Sandelic, D.-I. Stroe, and F. Iov, "Battery storage-based frequency containment reserves in large wind penetrated scenarios: A practical approach to sizing," *Energies*, vol. 11, no. 11, pp. 3065–3084, 2018.

[18] D. Stroe, V. Knap, M. Swierczynski, A. Stroe, and R. Teodorescu, "Operation of a grid-connected lithium-ion battery energy storage system for primary frequency regulation: A battery lifetime perspective," *IEEE Trans. Ind. App.*, vol. 53, no. 1, pp. 430–438, Jan. 2017.

[19] P. D. Reigosa, H. Wang, Y. Yang, and F. Blaabjerg, "Prediction of bond wire fatigue of igbts in a PV inverter under a long-term operation," *IEEE Trans. Power Electron.*, vol. 31, no. 10, pp. 7171–7182, Oct. 2016.

[20] Y. Yang, A. Sangwongwanich, and F. Blaabjerg, "Design for reliability of power electronics for grid-connected photovoltaic systems," *CPSS Trans. Power Electron. Appl.*, vol. 1, no. 1, pp. 92–103, Dec. 2016.

[21] M. Bost, B. Hirschl, and A. Aretz, "Effekte von eigenverbrauch und netzparität bei der photovoltaik," 2011. [Online]. Available: https://www.ioew.de/fileadmin/user_upload/BILDER_und_Downloaddateien/Publikationen/2011/Effekte_der_Netzparitt_-_Kurzfassung.pdf